Release of liposomes from hyaluronic acid-based hybrid systems: Effects of liposome surface and size

Céline Jaudoin, Maria Maue Gehrke, Isabelle Grillo, Fabrice Cousin, Malika Ouldali, Ana-Andreea Arteni, Evelyne Ferrary, Florence Siepmann, Juergen Siepmann, Fanny Simelière, et al.

Release of liposomes from hyaluronic acid-based hybrid systems: effects of liposome surface and size

Céline JAUDOIN [&a], Maria MAUE GEHRKE [&a], Isabelle GRILLO [#b], Fabrice COUSIN [#c], Malika OULDALI [d], Ana-Andreea ARTENI [d], Evelyne FERRARY [e, f], Florence SIEPMANN [g], Juergen SIEPMANN [g], Fanny SIMELIERE [a], Amélie BOCHOT [§a], Florence AGNELY [§a*]

[a] Université Paris-Saclay, CNRS, Institut Galien Paris-Saclay, 17 avenue des Sciences, 91400 Orsay, France.

[b] Institut Laue-Langevin, 71 avenue des Martyrs, 38042 Grenoble, France.

[c] Laboratoire Léon Brillouin, Université Paris-Saclay, UMR12 CEA-CNRS, 91191 Gif-sur-Yvette, France.

[d] Université Paris-Saclay, CEA, CNRS, Institute for Integrative Biology of the Cell (I2BC), 91198, Gif-sur-Yvette, France.

[e] Institut Pasteur, Universite Paris Cité, Inserm, Institut de l'audition, Technologies et thérapie génique pour la surdité, 63 rue de Charenton, 75012 Paris, France. evelyne.ferrary@inserm.fr

[f] APHP, GHU Pitié-Salpêtrière, Centre Implants auditifs, 50-52, bd Vincent Auriol, 75013 Paris, France

[g] Univ. Lille, Inserm, CHU Lille, U1008, F-59000 Lille, France.

[&]Same contribution. [#]Same contribution. [§]Same contribution

*Corresponding author, e-mail: florence.agnely@universite-paris-saclay.fr, telephone: +33 1 80 00 61 08

We would like, through this article, to pay tribute to the memory of Dr Isabelle Grillo.

Abstract

Mixtures of hyaluronic acid (HA, in the semi-dilute entangled regime) with liposomes (high lipid concentration) exhibit a great interest in drug delivery. Considering the difference of microstructures when varying the liposome surface, we aimed to determine if liposome characteristics (surface and size) also influenced their release from these hybrid systems and to explore the mechanisms involved. Small-angle neutron scattering, cryogenic electron microscopy, zetametry, and dynamic light scattering were used to characterize liposomes. The implemented Transwell® model (two compartments separated by a polycarbonate membrane) showed that both size and surface governed liposome release. At 150 nm, anionic liposomes with or without poly(ethylene glycol) chains (PEG) migrated from HA-liposome mixtures, while cationic and neutral ones did not. Furthermore, increasing the size of PEGylated liposomes up to 200 nm or more strongly hindered their migration. Below 200 nm, the smaller the liposome size, the faster the release. Multiple and complex mechanisms (interactions between HA and liposomes, water exchanges, liposome migration, swelling and erosion, and HA reptation) were involved. Their relative importance depended on liposome characteristics. The Transwell® model is a pertinent tool to assess in vitro the release of liposomes over several weeks and discriminate the formulations, depending on the foreseen therapeutic strategy.

Keywords: cryogenic electron microscopy; erosion; microstructure; migration; small angle neutron scattering; swelling.

Abbreviations: Chol, cholesterol; cryo-EM, cryogenic electron microscopy; D, day; DLS, dynamic light scattering; DSPE, 1,2-distearoyl-sn-glycero-3-phosphoethanolamine; EPC, egg phosphatidylcholine; HA, hyaluronic acid; HEPES, 4-(2-hydroxyethyl)piperazine-1-ethanesulfonic acid; Lip, neutral liposomes; Lip^-, anionic liposomes; Lip^+, cationic liposomes; LipPEG, PEGylated liposomes; PdI, polydispersity index; PEG, poly(ethylene glycol); PG, egg L-α-phosphatidylglycerol; SA, stearylamine; SANS, small angle neutron scattering.

Graphical abstract

1. Introduction

Nanomedicines can significantly impact human health for the prevention, diagnosis, and treatment of diseases (mainly cancer, infection, and pain) (Gonçalves et al., 2020; Hua et al., 2018; Uchegbu and Siew, 2013). Among them, liposomes play a leading role with more than 20 products commercialized (Crommelin et al., 2020). These biodegradable and deformable colloids are small vesicular structures (between 20 nm and a few µm) formed by phospholipid bilayers surrounding an aqueous core. They can encapsulate hydrophobic or hydrophilic molecules (Bozzuto and Molinari, 2015; Wang et al., 2012). Thus, they compensate for disadvantageous drug properties such as low solubility, degradation, and short half-life. They may also offer the possibility to sustain the release of drugs and address them to specific tissues by modifying the active molecule distribution (Agrahari et al., 2017). Their surface can easily be tuned by lipid composition, and their size can be controlled. However, in some cases, their instability can limit their industrial development (Shah et al., 2020).

Incorporating liposomes into concentrated polymer solutions or hydrogels is an efficient strategy to deliver drugs locally with or without injection. The benefits of this combination are to prolong the residence time of drugs at the site of administration, control their release for a more extended duration, and prevent the rapid elimination of both liposomes and drugs (El Kechai et al., 2016; Ensign et al., 2014; Grijalvo et al., 2016; Lajavardi et al., 2009; O'Neill et al., 2017). Hyaluronic acid (HA) is one of the most promising polymer candidates. This linear polysaccharide, found in animals and the human body, is mucoadhesive, biodegradable, and biocompatible. This negatively charged semi-rigid polyelectrolyte is soluble in water at neutral pH (Gatej et al., 2004; Lapčík et al., 1998). High molecular weight HA chains start to overlap at low concentrations to form a transient network (De Smedt et al., 1994; Krause et al., 2001).

The mixture of HA and liposomes offers many advantages. The dispersion of liposomes in HA is simple to manufacture. High drug concentrations can be achieved by increasing the proportion of liposomes in this hybrid system. Finally, the liposome composition can be adapted to the physicochemical properties of the drug and their size to the required application.

Knowledge of their microstructure is essential to control the use properties of such hybrid systems. In the work of El Kechai et al., (2017), we observed a microphase separation between liposomes and HA by confocal microscopy and freeze-fracture electron microscopy. In a more recent study (Jaudoin et al., 2022), we used small angle neutron scattering (SANS) to characterize the organization of mixtures composed of HA and 75 nm-liposomes with different surfaces (neutral, Lip, cationic, Lip^+, anionic, Lip^-, and decorated by poly(ethylene

glycol) chains, LipPEG). HA was in the semi-dilute entangled regime (1.5% (w/v), above the entanglement concentration C_e = 0.25 % (w/v)), and the liposome concentration was 80 mM lipids. Liposome surface governed the interactions and microstructure of these hybrid systems. Liposomes kept their integrity and assembled in clusters. For Lip^- and LipPEG, electrostatic and/or steric repulsions occurred between the vesicles and HA. It resulted in the formation of amorphous and dense clusters, probably by a depletion mechanism. Better dispersed and less dense aggregates were obtained with Lip^+ that can complex HA. With Lip, results were difficult to interpret due to their higher polydispersity.

In vivo, 150 nm-PEGylated liposomes were able to migrate through the HA transient network to reach and accumulate in the physiological membrane separating the middle and the inner ear after local injection (El Kechai et al., 2016).

Considering the difference of microstructures when varying the liposome surface, we were interested in determining if liposome characteristics also govern their release from hyaluronic acid-based hybrid systems. This work aimed to use a Transwell® model to assess the release of liposomes from HA-liposome mixtures over a long time (three weeks). We evaluated the effects of the surface of 150-nm liposomes and the size of PEGylated ones. To explore the mechanisms involved in liposome release, viscosity, volume variations of the formulations were also considered. The characterization of liposomes by dynamic light scattering (DLS), zetametry, cryogenic electron microscopy (Cryo-EM), and SANS was necessary to determine their inner structure and volume fraction before the release study. HA (1.5% (w/v)) and lipid (80 mM) concentrations were the same as reported before (Jaudoin et al., 2022).

2. Materials and methods

2.1. Materials

Sodium hyaluronate (HA) with a high molecular weight was provided by Acros Organics (M.W. supplier of 1.6 10^6 g/mol, batch A0375841, purity 95% Geel, Belgium). A weight average molar mass of 1.14 10^6 g/mol was determined by size exclusion chromatography coupled on-line with multiangle light scattering (Jaudoin et al., 2022). 1,2-distearoyl-sn-glycero-3-phosphoethanolamine-N-[methoxy-poly(ethyleneglycol)-2000] (DSPE-PEG_{2000}) and egg phosphatidylcholine (EPC, purity 96%) were provided by Lipoid GmbH (Ludwigshafen, Germany). Cholesterol (Chol), D_2O (99.9 atom % D), egg L-α-phosphatidylglycerol (PG), sodium chloride, stearylamine (SA), 4-(2-hydroxyethyl)piperazine-1-ethanesulfonic acid (HEPES) were obtained from Sigma-Aldrich Co. (St. Louis, USA). MilliQ water was used, with a resistivity of around 20 MΩ.cm (Millipore, Molsheim, France). All other chemicals were of analytical grade. The physical parameters of the different components of the formulations are detailed in Table S1.

2.2. Methods

2.2.1. Preparation and characterization of liposomes with different surfaces and sizes

Liposomes with different surfaces (neutral: Lip; positively charged: Lip^+; negatively charged: Lip^-; PEGylated: LipPEG) and LipPEG with different sizes (100, 150, 200, and 300 nm) (Table 1) were prepared by the thin-film hydration method as described previously (Bangham et al., 1965; Jaudoin et al., 2022). The lipid film was hydrated under vortex with HEPES/NaCl buffer (10/115 mM, pH 7.4) prepared either in H_2O or in D_2O. Suspensions were then extruded a few times (LIPEX Extruder, Evonik Nutrition & Care GmbH, Vancouver, Canada) through 0.8, 0.4, 0.2, and/or 0.1 μm polycarbonate filters to reach the targeted hydrodynamic diameter (D_h): 300, 200, 150 or 100 nm. After extrusion, lipids were quantified as described in Jaudoin et al. (2022). Briefly, EPC concentration was quantified by an enzymatic phospholipid assay (Biolabo SA, Maizy, France) after extrusion. Suspensions were diluted to perform absorbance measurements (500 nm) at 37 °C in the validity range of the assay (0.22–10.75 mM). On the assumption that the lipid ratio did not change during the different steps of liposome preparation, the total amount of lipids was calculated from the EPC concentration.

The final lipid concentration in liposome suspensions was adjusted to 80 mM for the Transwell® migration study and HA-liposome mixture manufacturing. The liposomes' hydrodynamic diameter and zeta (ζ) potential were determined in triplicate at 25 °C using a Zetasizer Nano ZS (Malvern, Worcestershire, UK) after dilution of the liposomal suspensions

to 2 mM of lipids with Milli-Q water using the experimental conditions reported in Jaudoin et al. (2022).

2.2.2. Cryogenic electron microscopy (cryo-EM) of 150 nm-liposomes with different surfaces

The cryo-EM grids were prepared using a Vitrobot Mark IV (ThermoFisher) at 20 °C and 100% humidity. Three μL of liposomes (Lip, Lip^+, Lip^-, LipPEG) in D_20 buffer were applied onto freshly glow-discharged Quantifoil grids (R2/2), 200 mesh grids and analyzed as in Jaudoin et al. (2022). Two to five hundred compiled measures of each type of liposomes were used to determine the liposome diameter D_{EM} and the mean number of shells per liposome N_s.

2.2.3. SANS data analysis of 150 nm-liposomes with different surfaces

SANS experiments were carried out on the PAXY instrument at Laboratoire Leon Brillouin (Saclay, France). q is the modulus of the scattering vector ($q = (4\pi/\lambda)\sin\theta$) with 2θ the scattering angle. To cover a q-range from 0.002 to 0.5 $Å^{-1}$, four configurations were used with the following wavelengths λ and sample-detector positions D (λ = 5 Å, D = 1 m; λ = 5 Å, D = 3.5 m; λ = 8 Å, D = 5 m; λ = 15 Å, D = 7 m). Liposomal suspensions (80 mM in D_2O buffer) were measured in 1 mm-path length rectangular quartz Hellma cells thermostated at 37 °C through a circulation water bath system. Data were corrected from the electronic background and empty cell. They were normalized to absolute scale (cm^{-1}) using standard procedures implemented in PAsiNET software at Laboratoire Leon Brillouin.

The SANS profiles of suspensions were analyzed using a method described by Nele et al. (2019). Since liposomes are spherical centrosymmetrical objects, the scattering intensity *I(q)* from suspensions exhibiting a multilamellar vesicle shape was defined as:

$$I(q) = \frac{\phi_{liposomes}}{V(R_N)} \times F^2(q) \times S(q) + I_{bck} \qquad \text{Eq. 1}$$

where

$$F(q) = (\rho_s - \rho_{solv}) \sum_{i=1}^{N} \left[3V(r_i) \frac{\sin(qr_i) - qr_i cos(qr_i)}{(qr_i)^3} - 3V(R_i) \frac{\sin(qR_i) - qR_i cos(qR_i)}{(qR_i)^3} \right] \qquad \text{Eq. 2}$$

for the solvent radius before shell i: $r_i = R_c + (i-1)(t_s + t_w)$ Eq. 3

and the shell radius for shell i: $R_i = r_i + t_s$ Eq. 4

With $\phi_{liposomes}$ the volume fraction of liposomes, *V(r)* the volume of a sphere of radius r, R_N the outer-most shell radius, *S(q)* the structure factor, R_c the radius of the core, t_s the thickness of the shell corresponding to the lipid bilayer, t_w the thickness of the solvent layer between the shells, ρ_s and ρ_{solv} respectively the scattering length densities of the shell and the solvent (whom difference is the contrast), *P(q)* the form factor that gives information on the particle size and shape, I_{bck} the contribution of the background signal (due for example to incoherent scattering in the case of neutrons). Radii are represented on Fig. S1.

The structure factor *S(q)* is the Fourier transform of the correlation pair function of centers of mass of the liposomes. By principle, $S(q)_{q\to\infty} = 1$. In case of dense formation of aggregates of liposomes, as observed in Jaudoin et al. (2022), there would be a correlation peak at $q^* \sim 2\pi/(2R_N)$ corresponding to the contact between liposomes in direct space, that give $q^* \sim 0.004$ Å^{-1} using the hydrodynamic diameter estimated by DLS. All others possible organizations (open aggregates, homogeneous distribution of centers of mass), would possibly give a correlation peak at larger distances, i.e. at even lower q than such a q^*. q^* almost corresponds to the minimal q ($q_{\min}$) probed in the experiment (only 3 experimental points are obtained at lower q). Therefore, in practice, all the potential features associated to *S(q)* are out of the q-window of the SANS that probes here the inner structure of liposomes. We have then set the value of *S(q)* at 1 for every q during fitting.

2.2.4. Calculation of volume fractions of 150 nm-liposomes with different surfaces

Liposome volume fractions were estimated by calculation using cryo–EM and SANS data. For each type of liposomes at D_h = 150 nm, the mean number of shells per vesicle N_s was determined on cryo–EM images (200–500 counts/kind of liposomes). Two classes of liposomes were defined: the unilamellar and oligolamellar (> one bilayer) vesicles. To simplify the calculations, oligolamellar vesicles were considered bilamellar ones. The lipid shell volume of the bilayer of uni- (V_U *(shell)*) and bi-lamellar (V_B *(shell)*) vesicles were determined as follows:

$$V_U(shell) = V(R_{EM}) - V(R_{EM} - t_s) \text{ and} \quad \text{Eq. 5}$$

$$V_B(shell) = V(R_{EM}) - V(R_{EM} - t_s) + V(R_{EM} - t_s - t_w) - V(R_{EM} - 2t_s - t_w) \quad \text{Eq. 6}$$

with R_{EM} the liposome radius measured on cryo–EM images. Knowing the lipid density for each type of liposomes (0.994 g/cm^3 for Lip$^+$ and 1.01 g/cm^3 for others, detailed in supplementary material Table S1), the mass of lipids necessary to build one object, uni- or

bilamellar (m_U and m_B, respectively), was calculated. The number of liposomes per volume unit (n) and the liposome volume fraction $\phi_{liposomes}$ were determined as follows:

$$n = \frac{C_{lipids}}{f_U m_U + f_B m_B} \text{ and } \phi_{liposomes} = n \times V(R_{EM}) \qquad \text{Eq. 7 and Eq. 8}$$

with f_u and f_B the frequency of uni- and bilamellar vesicles, respectively, C_{lipids} the mass concentration of lipids. For LipPEG, the outer corona of PEG_{2000} of thickness t_{PEG} ~4.5 nm (Kenworthy et al., 1995) was taken into account to calculate the volume fraction:

$$\phi_{LipPEG} = n_{LipPEG} \times V(R_{EM} + t_{PEG}) \qquad \text{Eq. 9}$$

2.2.5. Preparation of HA liposomal mixtures and HA solutions

HA-liposomes (HA-Lip, HA-Lip$^+$, HA-Lip$^-$, or HA-Lip PEG) were prepared by dissolving HA at 1.5% (w/v) in the corresponding liposome suspension in H_2O buffer (HEPES/NaCl 10/115 mM) at the lipid concentration of 80 mM. After vortexing for 10 min, mixtures were maintained at room temperature for 1 h, and finally manually stirred for 30 s. A vacuum pump was used to remove bubbles, and samples were kept at 4 °C for at least 12 h before use. The osmolality of the hybrid systems was comprised between 289 and 304 mOsm/kg (Roebling osmometer, Berlin, Germany). Two or 3 mL of HA-liposomes were prepared for Transwell® and rheology studies, respectively.

2.2.6. Rheology measurements

Flow measurements were performed in triplicate on 3 batches of HA-LipPEG (100, 150 and 200 nm) and HA solution at 1.5% (w/v) in H_2O buffer, using a rotational rheometer ARG2 (TA instruments, New Castle, USA) equipped with an aluminum cone/plate geometry (diameter 4 cm, angle 1° and cone truncation 28 μm). After 2 min of equilibration at 37 °C, the shear rate was increased from 0.01 to 1000 s^{-1}, maintained at 1000 s^{-1} for 2 min, and then decreased down to 0.01 s^{-1}. Rheograms were fitted according to the Williamson equation (Eq. 10) (Milas et al., 2002) using TRIOS software (TA instruments – Waters LCC, New Castle, USA) to determine the zero-shear rate viscosity η_0.

$$\eta = \frac{\eta_0}{1 + (k\dot{\gamma})^n} \qquad \text{Eq. 10}$$

with k (s) the consistency, $\dot{\gamma}$ the shear rate (s^{-1}) and n the power law index. This model is suitable to describe a shear-thinning behavior with a plateau at a low shear rate. We also

reanalyzed previous rheograms of HA-Lip, HA-Lip^{+}, and HA-Lip^{-} (D_h = 150 nm) from El Kechai et al. (2015) with the Williamson equation.

2.2.7. Release of liposomes using a Transwell® model

The release of liposomes with different surfaces (Lip, Lip^{+}, Lip^{-} and LipPEG) and Lip PEG with different sizes (100, 150, 200, and 300 nm) from HA-liposomes in H_2O buffer was evaluated in triplicate for each formulation on Costar® Transwell® (Corning, Kennebunk, USA) at 37 °C.

The Transwell® model consisted of two compartments separated by a polycarbonate membrane (thickness: 10 µm; surface area: 0.33 cm²; diameter: 6.5 mm) (Fig. 1). This semi-permeable membrane had cylindrical pores (pore tortuosity: 1) with controlled density (2.10^6 pores/cm²) and width (3 µm), according to technical data given by the supplier.

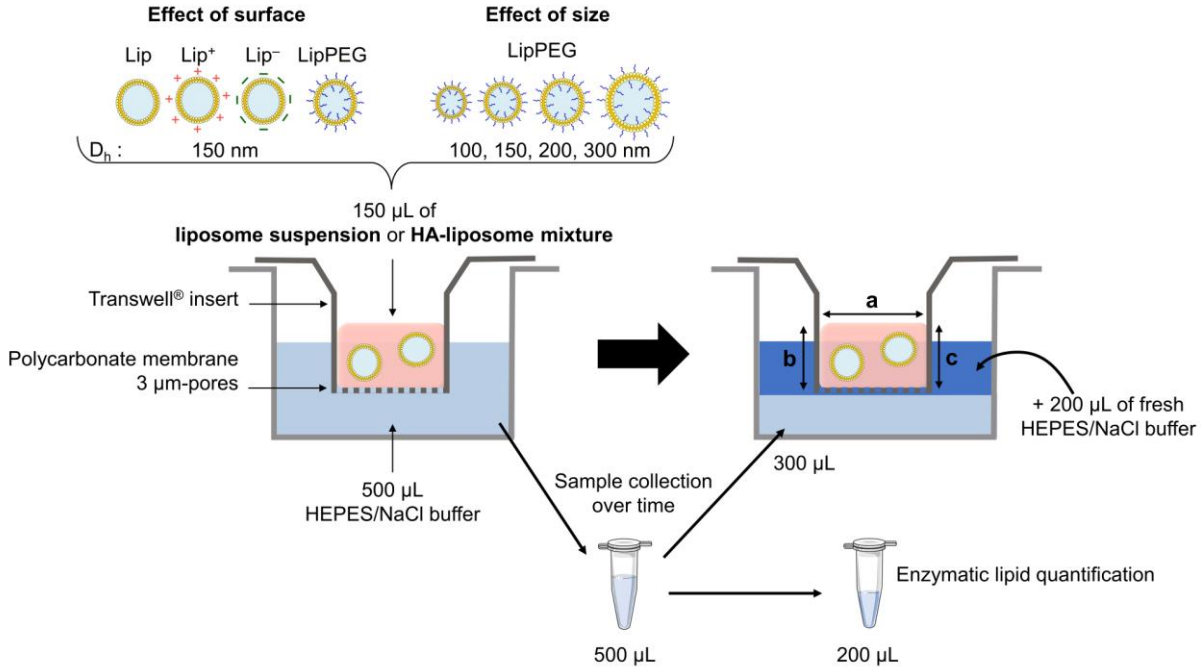

Fig. 1. Sampling protocol using a Transwell® model

To verify that the 3 µm pore size membrane was non-limiting for liposome migration, suspensions at 80 mM lipids were also studied (Lip, Lip$^{+,}$ and LipPEG with different sizes: 150, 200, and 300 nm).

A 0.4 µm pore-size membrane (thickness: 10 µm; surface area: 0.33 cm²; diameter: 6.5 mm, pore tortuosity: 1, 1.10^8 pores/cm²) was also used as a limiting membrane to contribute to understanding HA-liposome behaviors (with 150 nm-Lip, Lip^{+}, and LipPEG).

– *Release from HA-liposome mixtures*

150 µL of each formulation (liposomes or HA-liposomes) and 500 µL of HEPES/NaCl buffer in H_2O were placed respectively in the upper (donor) and lower (receptor) compartments of each well (n = 3). The HEPES/NaCl buffer osmolality in the receptor compartment was equivalent to that of the studied formulation (10/115 mM for suspensions and 10/145 mM for HA-liposomes). In this way, water exchanges through the membrane due to osmotic pressure should be limited. To prevent evaporation, the 24-well plate was sealed with adhesive tape (Scotch® crystal tape, 3M, Cergy-Pontoise, France). The plate was placed inside an oven at 37 °C. The lipid concentration in the receptor compartment was quantified at different times t:

- For suspensions: 30 min, 2, 4, 6, 24, 30, 48, 54, 72, and 78 hours and 7, 8, 9, and 10 days.
- For HA-liposomes: 6, 24, 30, 48, 54, 72 and 78 hours and 7, 8, 10, 14, 21 days.

At each time *t*, the entire content of the receptor compartment was removed and weighed (detailed protocol in Fig. 1). 300 µL of the original content were replaced in the receptor compartment, and 200 µL were kept at 4 °C for enzymatic lipid quantification (see section 2.2.1). Then, the content of the receptor compartment was adjusted to 500 µL with fresh buffer. The cumulated amount of lipids released was expressed as a percentage (Eq. 11):

$$\%\ lipids = \frac{\sum_{t=0}^{t} n_t}{n_0} \qquad \text{Eq. 11}$$

with n_t the amount of lipids in the receptor compartment (moles) at collection time t, and n_0, the total amount of lipids (moles) in the donor compartment at initial time t_0. The liposome size distribution was checked in the receptor compartment for 150-nm Lip, 150-nm $Lip^{+,}$ and 300 nm-LipPEG at 30 min and HA-150 nm-LipPEG at 6, 24, 30, and 48 h by dynamic light scattering as described in section 2.2.1 but without dilution.

– *Volume of HA liposomal mixtures*

The volume of HA-liposome mixtures was measured over time. Pictures of the donor compartment were taken at each time point for each well (n = 3). The characteristic lengths of the hybrid systems (*a*, *b* and *c*) (Fig. 1) were measured using the ImageJ software. The percentage of volume at time t of the formulation in the Transwell® insert was calculated according to Eq. 12 and 13:

$$\%\ volume = \frac{V_t}{V_0} \times 100 \qquad \text{with } V_t = \frac{\pi}{8} a^2 (b_t + c_t) \qquad \text{Eq. 12 and 13}$$

with V_t (mm^3) the volume of HA-liposomes in the insert, V_0 (mm^3) this volume at initial time t_0, and a, b_t, and c_t (mm) the characteristic lengths of the systems in the donor compartment at time t (Fig. 1).

To better understand the mechanisms involved in the liposome release, the same protocol was applied using the 0.4 µm pore-size Transwell® membrane to measure the volume of HA-liposomes (HA-Lip, HA-Lip$^+$, HA-Lip$^-$ and HA-LipPEG at 150 nm) over time. This membrane strongly limited liposome release, independently of liposome surface.

3. Results

3.1. Characterization of liposomes and determination of their volume fraction

Lipids and their ratios were chosen according to the ones commonly used in conventional liposome formulations. The physico-chemical characteristics of the liposome suspensions are summarized in Table 1.

As SANS required the use of D_2O for contrast reasons we checked that the change from D_2O buffer to H_2O buffer did not modify liposome characteristics. Liposomes obtained either in H_2O or D_2O buffers exhibited similar hydrodynamic diameter and ζ potential values, as expected for systems mainly governed by electrostatic interactions (Jaudoin et al., 2022). All formulations reached the targeted hydrodynamic diameter with a narrow size distribution, except 300 nm-LipPEG that were slightly more polydisperse than the others. The ζ potential of these suspensions were in accordance with the charge of the lipids used for their preparation.

As previously observed and discussed with smaller liposomes of 75 nm (Jaudoin et al., 2022), DLS diameters were larger than cryo-EM ones. Many liposomes were oligolamellar at 150 nm, and some were distorted, probably due to their high concentration (80 mM lipids) (Fig. 2A, Table 1).

By contrast with 75 nm-liposomes, SANS profiles of 150 nm liposomes did not accurately assess liposome size as it was too large to observe a plateau at low q. Along the same lines, the q_{min} of the experimental q-window is too large to probe any possible features associated with the existence of a structure factor (see materials and methods). Nevertheless, important differences were noticeable depending on the liposome surface (Fig. 2B). Lip showed a peak at q = 0.1 $Å^{-1}$ characteristic of oligolamellar vesicles (Fig. 2B) and the highest percentage of liposomes with several bilayers (Table 1). Lip$^+$ and Lip$^-$ SANS profiles were relatively close (Fig. 2B) whereas LipPEG displayed two distinct peaks.

The mean number of lipid bilayers per liposome ($\overline{N}_s$) and their respective frequencies determined by cryo-EM images were included in the fitting of SANS data with a multilamellar model (Table S2) to determine the bilayer thickness (t_s), and the water thickness between bilayers (t_w) (Table 1). t_s was similar whatever the formulation, but t_w depended on the liposome surface (Table 1). Compared to neutral liposomes (2.5 nm), the gap was more significant when there were electrostatic repulsions between the bilayers (Lip^- and Lip^+, 3.8 nm) and even more when combining electrostatic and steric repulsions (LipPEG, 9.6 nm). For this latter system the thickness was approximately twice the theoretical thickness of PEG2000 layer (~4.5 nm), which was not visible by SANS for contrast reasons since the PEG brush is highly solvated. The PEG2000 brushes were face-to-face between the bilayer.

In the liposome suspensions studied by cryo-EM, oligolamellar vesicles were predominantly bilamellar, which justified the use of this approximation for volume fraction calculations (section 2.2.4). Liposome volume fractions in D_2O ranged between 19 and 24%, indicating liposomes occupied a significant volume in the HA-liposome mixtures.

Considering the similar characteristics of liposomes in both buffers by DLS and zetametry, the rest of the experiments were performed solely in H_2O buffer and we assumed similar volume fractions as in D_2O.

Table 1: Characteristics of liposomes prepared in D_2O and H_2O buffers.

Name *Lipid composition* *Lipid ratio* *(mol%)*	**H_2O/D_2O**	**Targeted D_h**	**Electrophoretic mobility/DLS** *25 °C,* *[Lipids] = 2 mM*			**Cryo–EM**							**SANS** *37 °C,* *[Lipids] = 80 mM*				$\phi_{liposomes}$
			D_h by intensity (nm)	PdI	ζ potential (mV)	D_{EM} (nm)	PdI	N_s Frequency (%) 1	2	3	4	[5–12]	t_s (nm)	PD ratio of t_s	t_w (nm)	PD ratio of t_w	
Lip *EPC:Chol* *65:35*	D_2O	150	152 ± 17	0.05	–3 ± 1	112 ± 39	0.16	50	32	8	6	4	3.9	0.11	2.5	0.20	0.19
	H_2O	150	161 ± 24	0.09	–6 ± 4												
Lip$^+$ *EPC:Chol:SA* *55:35:10*	D_2O	150	153 ± 29	0.14	+66 ± 1	142 ± 64	0.20	53	37	7	2	0	3.8	0.12	3.8	0.35	0.23
	H_2O	150	143 ± 25	0.12	+53 ± 10												
Lip$^-$ *EPC:Chol:PG* *55:35:10*	D_2O	150	153 ± 35	0.20	–65 ± 2	97 ± 72	0.40	66	26	5	2	1	3.8	0.10	3.8	0.50	0.19
	H_2O	150	153 ± 21	0.08	–53 ± 9												
LipPEG *EPC:Chol:DSPE-PEG_{2000}* *60:35:5*	D_2O	150	149 ± 34	0.20	–34 ± 1	97 ± 43	0.19	55	38	5	2	0	3.9	0.12	9.6	0.24	0.24
	H_2O	100	104 ± 16	0.09	–27 ± 9												
		150	155 ± 27	0.11	–32 ± 6												
		200	201 ± 45	0.21	–22 ± 4												
		300	290 ± 75	0.26	–25 ± 5												

D_h: hydrodynamic diameter, DLS: dynamic light scattering, cryo–EM: cryogenic transmission electron microscopy, N_s: shell number per liposomes, t_s: thickness of the shell, t_w: thickness of the solvent layer between the shells, $\phi_{liposomes}$: liposome volume fraction of the suspension at 80 mM

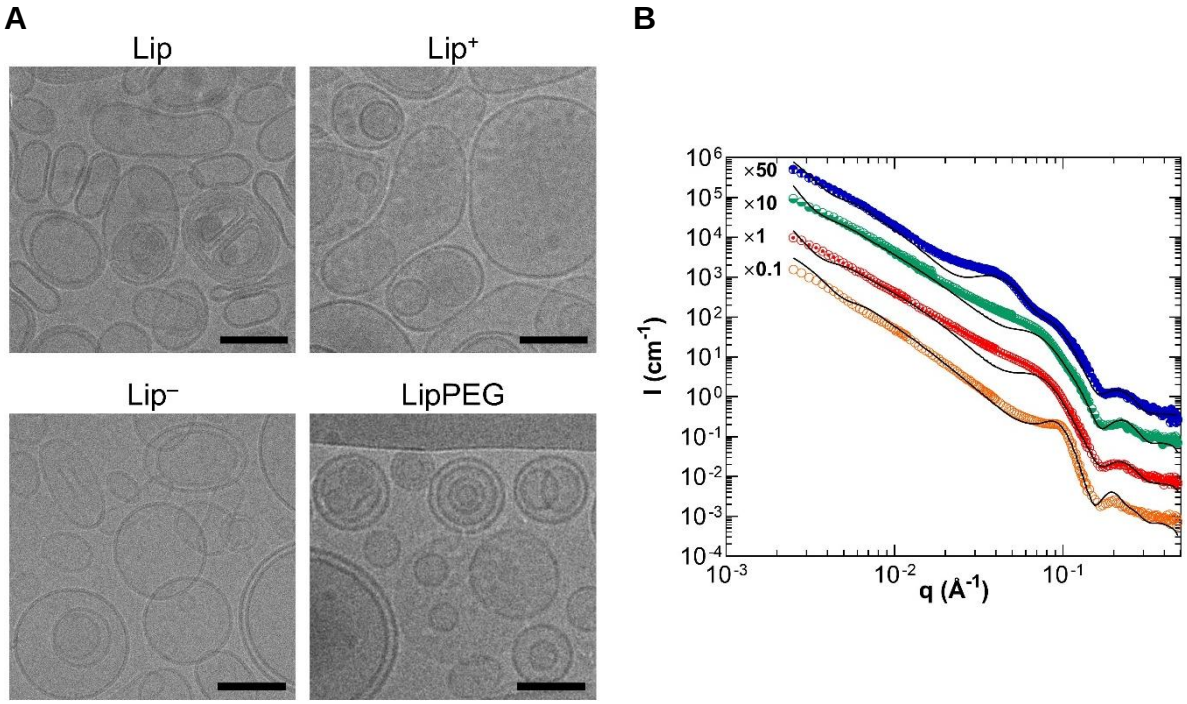

Fig. 2: A. Cryo-EM pictures of liposome suspensions in D_2O buffer (HEPES/NaCl 10/115 mM, pH 7.4), D_h = 150 nm. Scale bar = 100 nm. **B.** Effect of surface on the scattering intensity from 150 nm-suspensions. For D_h = 150 nm: Lip (○), Lip^+ (⊙), Lip^- (◒), LipPEG (◒). Bests fits from SANS data analysis are represented in full lines. [Lipids] = 80 mM, T = 37 °C, D_2O buffer (HEPES/NaCl 10/115 mM, pH 7.4).

3.2. Viscosity of HA-liposome mixtures

As the viscosity is likely to influence the release of liposomes, a rheological study was performed at 37°C. A shear thinning behavior was obtained and the viscosity at zero-shear rate η_0 was determined as a function of liposome surface (150 nm) and liposome size (LipPEG). Due to batch-to-batch variation of its molecular weight, HA concentration was adjusted so that the viscosity of HA solutions was equivalent between the present study (1.5% (w/v), M.W. supplier = 1.6 10^6 g/mol) and that of El Kechai et al. (2015) (2.28% (w/v), M.W. supplier = 1.5 10^6 g/mol). As demonstrated earlier by El Kechai et al. (2015), the incorporation of liposomes at 80 mM increased the viscosity compared to HA alone. The η_0 viscosity varied with liposome surface: $\eta_{0\ HA\text{-}LipPEG} > \eta_{0\ HA\text{-}Lip^-} > \eta_{0\ HA\text{-}Lip^+} \approx \eta_{0\ HA\text{-}Lip}$ (Fig. 3) and was dramatically higher than that of water (5 orders of magnitude). An increase or decrease in LipPEG size of 50 nm resulted in a decrease in HA-LipPEG viscosity of approximately 20 to 30%, respectively.

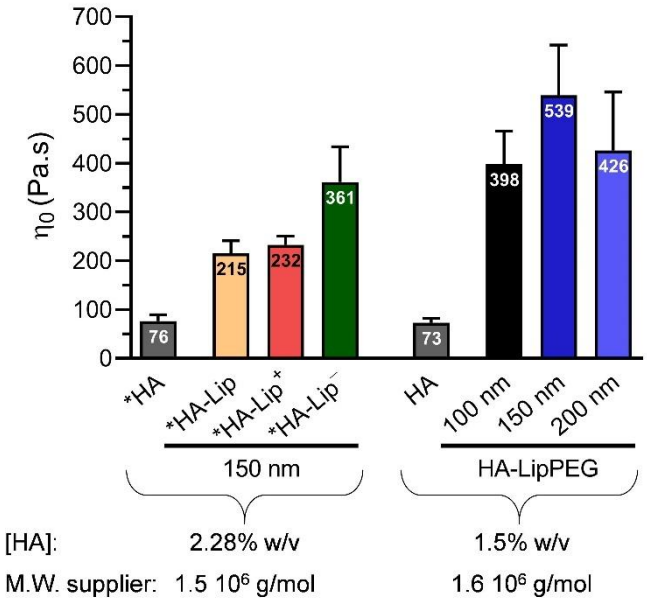

Fig. 3. Zero-shear viscosities (η_0) of HA solution and HA-liposome mixtures in H_2O buffer, as a function of liposome surface (D_h = 150 nm) and liposome size (HA-LipPEG). T = 37 °C, [Lipids] = 80 mM. Results are means ± standard deviation (n = 3). *Data from El Kechai et al. (2015) re-analyzed with the Williamson equation.

3.3. Liposome release study from HA-liposomal mixtures using a Transwell® system

3.3.1. Effect of Transwell® membrane pore size

Two polycarbonate membranes with 3 or 0.4 μm pores were first used to quantify the release at 37°C of 150 nm-liposomes from suspensions at 80 mM without HA. The lipids recovered in the receptor compartment were recorded over time (Fig. S2). At 6 hours, less than 3 % of the lipids were released with the 0.4 μm pore size compared to more than 60 % with the 3 μm one, for which the liposome migration to the receptor compartment was fast, whatever their surface (Fig. S2B) and size (Fig. S2C). Liposomes were not distorted when passing through this polycarbonate membrane (Fig. S3A, no effect on size distribution). Therefore, the 3 μm pore-size membrane was considered non-limiting and was selected to assess the effects of liposome surface and size on their release from the hybrid systems. In contrast, the 0.4 μm membrane strongly impeded the 150 nm-liposome migration and was used as a limiting membrane to also contribute to understanding HA-liposome behaviors.

When liposomes were incorporated in 1.5 % HA, release kinetics were dramatically slowed (Fig 4, Table 2). The release's extent depended on the liposome's surface and the size of PEGylated ones (see sections 3.3.2 and 3.3.3).

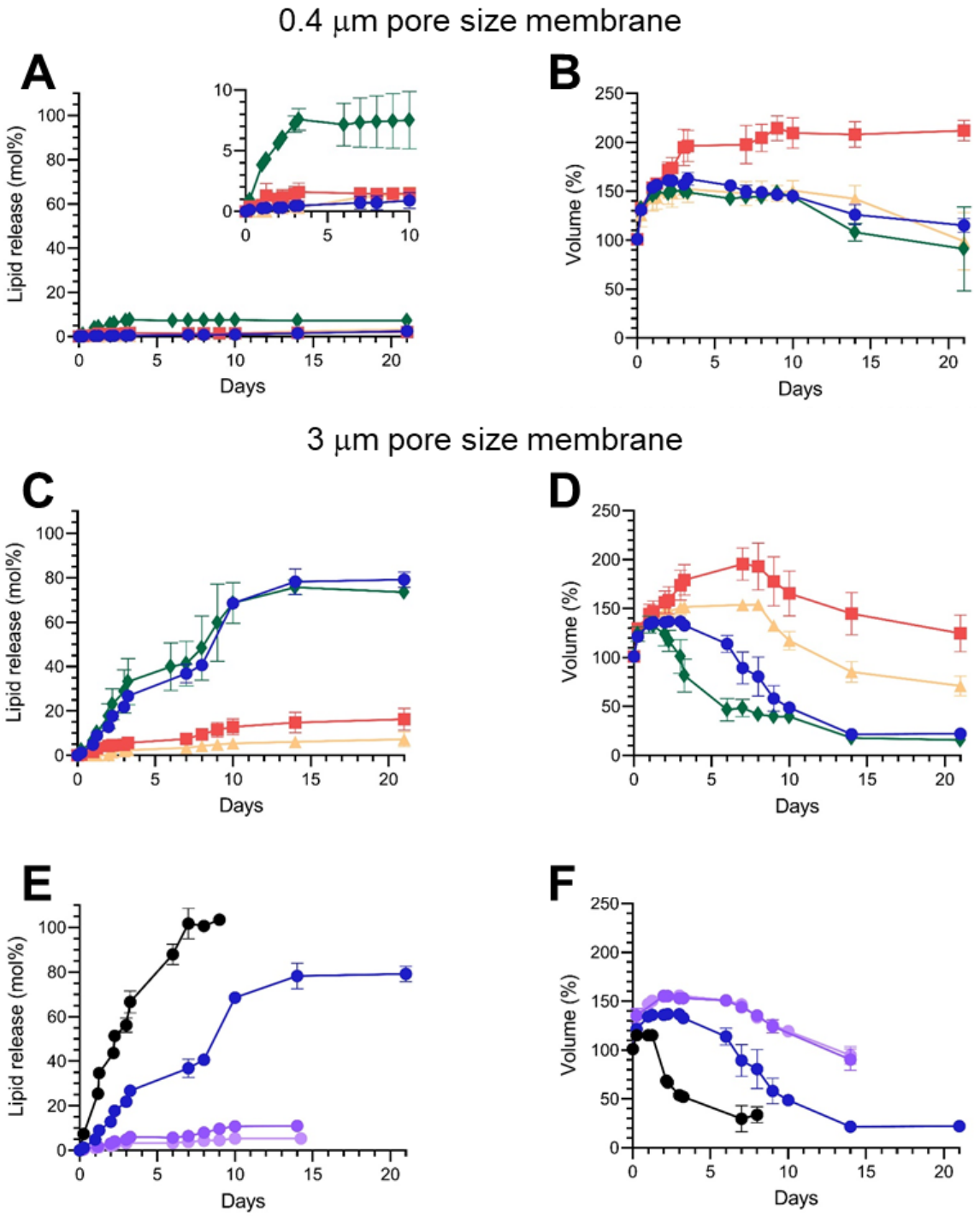

Fig. 4. A Transwell® study of HA-liposome mixtures at 37 °C using limiting (0.4 µm pores) **(A, B)** or non-limiting (3 µm pores) **(C, D, E, F)** membranes. **(A, B, C, D)** Effect of liposome surface (D_h = 150 nm): HA-Lip (▲), HA-Lip$^+$ (■), HA-Lip$^-$ (♦), and HA-LipPEG (●). **(E, F)** Effect of LipPEG size: 100 nm (●), 150 nm (●), 200 nm (●) and 300 nm (●). **(A, C, E)** Lipid release (mol%) in the receptor compartment of the Transwell® over time. **(B, D, F)** Volume (%) of HA-liposome systems in the donor compartment over time. The insert in figure A zooms at short times. Results are means ± standard deviation (n = 3). Nota bene: For all

release profiles, a slower release step was observed between D_3 and D_7. This phenomenon might be due to the sampling schedule spaced during this period.

Table 2. Parameters characterizing the release at 37 °C of liposomes from HA-liposome mixtures using a Transwell® system with non-limiting (3 μm) or limiting (0.4 μm) membranes (n = 3).

		3 μm-pore size							**0.4 μm-pore size**			
Liposome	Liposome size (nm)	$t_{10\%}$	$t_{50\%}$ (days)	$t_{75\%}$	Total lipid release (mol%)	V_{max} (%)	t_{max} (days)	*[HA]'* % (w/v)	Total lipid release (mol%)	V_{max} (%)	t_{max} (days)	*[HA]'* % (w/v)
Lip	150	28	*n.a.*	*n.a.*	7 ± 3 at D_{21}	154 ± 5	8.0	0.97	3 ± 1 at D_{21}	152 ± 14	3.2	0.99
Lip^+	150	8.2	*n.a.*	*n.a.*	16 ± 5 at D_{21}	195 ± 16	7.0	0.77	2 ± 1 at D_{21}	214 ± 13	9.0	0.70
Lip^-	150	1.2	8	14	75 ± 1 at D_{21}	134 ± 9	1.0	1.12	7 ± 2 at D_{21}	150 ± 4	3.0	1.00
LipPEG	100	0.4	2.2	4.5	103 ± 5 at D_9	115 ± 3	1.0	1.30	*n.d.*	*n.d.*	*n.d.*	*n.d.*
	150	1.5	9	13	79 ± 4 at D_{21}	137 ± 4	2.2	1.10	2 ± 1 at D_{21}	163 ± 6	3.2	0.92
	200	9	*n.a.*	*n.a.*	11 ± 1 at D_{14}	155 ± 6	2.0	0.97	*n.d.*	*n.d.*	*n.d.*	*n.d.*
	300	*n.a.*	*n.a.*	*n.a.*	5 ± 1 at D_{14}	156 ± 4	3.0	0.96	*n.d.*	*n.d.*	*n.d.*	*n.d.*

$t_{10\%}$, $t_{50\%}$ and $t_{75\%}$: time to achieve respectively 10%, 50% and 75% of lipid released in the receptor compartment; D: day. V_{max}: maximum volume reached by the HA-liposome mixture in the donor compartment; t_{max}: time at V_{max}; [HA]': theoretical HA concentration in the donor compartment at V_{max} supposing that HA did not cross the membrane. At t_0, [HA] was 1.5% (w/v). *n.a.:* not applicable; *n.d.:* not determined.

Images of the HA-liposomes in the donor compartment were taken over time (Fig. S4). With the limiting membrane, macrophase separation with transparent areas without liposomes appeared and was visible for all the formulations (Fig. S4C) at D_{14} and D_{21}. In contrast, it was not systematically observed when using the non-limiting membrane. Whatever the pore size, a zone depleted in liposomes appeared over time above the membrane for HA-Lip$^+$.

From the images, the volume of HA-liposomes in the donor compartment was recorded over time (Fig. 4B, D, F). HA-liposome volume increased rapidly up to a maximal value, V_{max} (Table 2). This volume expansion was slightly higher with the limiting membrane (Fig. 4B) than with the non-limiting one (Fig. 4D) and was followed by a plateau or a volume shrinkage, much more pronounced with the 3 μm pore-size membrane.

3.3.2. Effect of the surface of 150 nm-liposomes using the 3 μm pore-size membrane

The liposome surface strongly influenced the liposome delivery from the hybrid systems (Fig. 4C). Two distinct behaviors were observed: systems that could release liposomes (HA-Lip$^-$ and HA-LipPEG) and those that could barely not (HA-Lip and HA-Lip$^+$). Indeed, around 75% of the lipids were released at D_{14} for anionic and PEGylated HA-liposomes (HA-Lip$^-$ and HA-LipPEG) compared to less than 20% for HA-Lip and HA-Lip$^+$ (Table 2). For HA-Lip$^-$ and HA-LipPEG that presented similar release profiles, lipids were quantified in the receptor compartment as early as 6 hours after the beginning of the experiment. The liposome release was extended over time (several days) with 50% of lipid release at D_8–D_9. Interestingly, the size distribution of LipPEG was not modified during the release (Fig. S3B), suggesting that liposomes were altered neither in the mixture nor during their migration to the receptor compartment.

At D_{14}, HA-Lip$^-$ and HA-LipPEG had almost disappeared from the donor compartment, while HA-Lip and HA-Lip$^+$ still occupied a significant volume (Fig. S4A). However, at D_{14}, these latter systems were no more homogenous.

In less than one day, the volume of HA-liposomes increased rapidly by more than ~35%, independently of liposome surface. After D_1, each system displayed a different volume expansion profile (Fig. 4C). V_{max} varied with the liposome surface (Table 2): $V_{max\ HA\text{-}Lip+} > V_{max\ HA\text{-}Lip} > V_{max\ HA\text{-}LipPEG} \approx V_{max\ HA\text{-}Lip–}$. For systems releasing a low amount of lipids (HA-Lip and HA-Lip$^+$), their volumes progressively increased to reach a maximum at D_7–D_8. For systems able to release liposomes (HA-Lip$^-$ and HA-LipPEG), their volumes attained their maximum volume around D_1–D_2. For all formulations, after the maximum was

reached, the HA-liposome volume started to decrease. This volume shrinkage started at D_2–D_3 for systems releasing liposomes. It was faster for HA-Lip$^-$ than for HA-LipPEG. However, their lipid releases were similar (Fig. 4D). For systems that released a low amount of lipids, the HA-liposome volume decreased progressively around D_9. However, it was lower for HA-Lip$^+$ than for other systems up to 21 days.

Comparatively, when using the limiting 0.4 μm pore-size membrane, volume shrinkage was slower and occurred to a lower extent (HA-Lip, HA-Lip$^-$ and HA-LipPEG), if not inexistent (HA-Lip$^+$) (Fig. 4B).

3.3.3. Effect of liposome size using the 3 μm pore-size membrane

In pharmaceutical applications, hydrophilic drugs can be encapsulated in the aqueous core of the vesicle and the maximum drug loading strongly depends on the size of the liposomes. Furthermore, size can be a crucial parameter since it is directly correlated with the diffusion coefficient of particles. LipPEG were selected among the formulations mentioned above to conduct this study because 150-nm LipPEG migrated rapidly.

The liposome size had a substantial impact on the LipPEG release from HA-LipPEG. Indeed, the Transwell® system allowed distinguishing two categories of HA-LipPEGs: those that released liposomes (100 and 150 nm-LipPEG) and those that practically did not (200 and 300 nm-LipPEG) (Fig. 4E). The smallest LipPEG size (100 nm) exhibited a higher rate and extent of lipid release from HA-LipPEG. HA-100 nm-LipPEG released 100% of its lipid content into the receptor compartment in 7 days (Table 2). In contrast, the release was strongly hindered when the size was larger than or equal to 200 nm. Less than 15% of total lipids were recovered in the receptor compartment over 14 days from HA-200 nm and 300 nm-LipPEG mixtures, respectively.

The effect of LipPEG size on the macroscopic aspect (Fig. S4) and the volume (Fig. 4F) of HA-LipPEG in the donor compartment was evaluated over time. All HA-LipPEG formulations remained homogenous during the release. However, changes in the volume of HA-LipPEG were noticeable over time and between the different LipPEG sizes studied (Fig. 4F). The maximum volume reached by HA-100 nm-LipPEG was lower than for 150 nm-LipPEG (Table 2). Contrarily, for mixtures that did not release liposomes (HA-200 nm-LipPEG and HA-300 nm-LipPEG), their volumes increased by approximately 50% compared to their initial volumes with superposable profiles, despite their difference in liposome size. For all sizes, after this expansion step, a decrease in HA-LipPEG volume occurred in the

donor compartment. This shrinkage was faster and started earlier when the LipPEG size was smaller (Fig. 4F), but was similar for 200 and 300 nm LipPEG.

4. Discussion of the release mechanisms

The Transwell® model enabled us to efficiently assess in vitro liposome release from HA-liposome systems at a long time scale (a few weeks) and discriminate them, which was the main objective of this work. The synthetic membrane of this device was not intended to mimic a biological membrane, but to allow comparing the behavior of the different hybrid systems.

Both, size (for PEGylated liposomes) and surface (for D_h = 150 nm) influenced liposome release. Some systems released at least 80% of their lipid content in 1 to 2 weeks (HA-150 nm-Lip$^-$, HA-100 nm-LipPEG, and HA-150 nm-LipPEG), while others released less than 16% over 3 weeks (HA-150 nm-Lip, HA-150 nm-Lip$^+$, HA-200 nm-LipPEG, and 300 nm-LipPEG).

Although the release rate increased with a decrease in LipPEG size, suggesting a mechanism of diffusion (Fig. 4B), it was probably not the sole driving force. Indeed, no proportionality was observed between the cumulative amount of liposome released and the square root of time, as it would be expected for Fickian diffusion with constant diffusivity and stationary boundary conditions for the given geometry (Ritger and Peppas, 1987). Moreover, the most viscous HA-liposome mixtures (HA-Lip$^-$ and HA-LipPEG, Fig. 3) showed the fastest release (Fig. 4), which would not be expected if diffusional mass transport was dominant. Besides, in earlier work, we evaluated liposome mobility within HA-liposomes over a short time period (a few ms) by single-particle tracking coupled with videomicroscopy (El Kechai et al., 2017). It differed according to their surface (HA-LipPEG ≈ HA-Lip$^-$ > HA-Lip > HA-Lip$^+$) and was not described by a Brownian motion.

To better understand the mechanisms involved in liposome release, we focused on the different HA/liposome interactions that might affect their diffusion in HA solutions. Lip$^+$ might complex with negatively charged HA chains via electrostatic attractions (El Kechai et al., 2017), whereas Lip might bind to hydrophobic regions along the HA chain (Taglienti et al., 2006), leading to their immobilization within the formulations. Indeed, clusters of contiguous CH groups are present on the secondary structure of HA chains, forming hydrophobic areas that could bind to lipidic membranes such as the one of Lip (Scott, 2007). On the contrary, Lip$^-$ and LipPEG, both negatively charged, are released from HA-liposome mixtures. Their negative charge providing electrostatic repulsions with the anionic

carboxylate groups of HA or steric protection for LipPEG, could promote HA chain rearrangement and liposome diffusion.

As previously shown with 75 nm- (Jaudoin et al., 2022) and 150 nm-liposomes (El Kechai et al., 2017), the above-mentioned interactions impacted the HA-liposome microstructure. It might, thus, influence the release of liposomes. Macroscopically, HA-liposome hybrid systems were homogenous at t_0. But at the microscale, anionic liposomes (Lip^- and LipPEG) formed dense clusters where they were in close contact, contrary to Lip^+ that might be coated by HA (Jaudoin et al., 2022). At the concentration of 1.5%, $C > C_e$ = 0.25% (w/v), HA chains were entangled and formed a network characterized by a mesh size of 7 nm (Jaudoin et al., 2022), far below the size of the liposomes. This mesh size in HA-liposome systems is likely to be even smaller than 7 nm, due to the exclusion of HA chains from the volume occupied by liposomes (depletion effect). This exclusion increases locally the HA concentration, which is consistent with the viscosity enhancement (Fig. 3). Consequently, individual liposomes were not caged within HA meshes but were aggregated in clusters within the HA network, in accordance with El Kechai et al., 2017. The high viscosity and viscoelasticity of the systems resulting from both, a HA concentration > C_e and elevated liposome volume fraction, dramatically slowed down the dynamics, thereby allowing for kinetic stability. The viscosity differences depending on liposome surface (Fig. 3) can be explained by the contribution of both, the depletion mechanism of entropic origin and the interactions between liposomes and HA mentioned above. When repulsive interactions occurred (Lip^- and LipPEG), the segregative behavior was reinforced, and the viscosity was highest. With Lip and Lip^+, the attractive interactions counterbalanced the depletion effect, limiting the exclusion of HA chains and, consequently, the viscosity enhancement.

During the release, the microstructure of HA-liposomes evolved. Indeed, changes were noticed macroscopically in the donor compartment. Areas free of liposomes observed in HA-Lip and HA-Lip^+ (Fig. S4A) suggested that a macrophase separation occurred in these systems.

When using a limiting membrane (0.4 μm pores), macrophase separation was visible for all formulations (Fig. S4C). Concerning HA-Lip^+, the polycarbonate membrane, which is negatively charged (Kirby and Hasselbrink, 2004), might have attracted the Lip^+ present at proximity creating a depleted area observed with both limiting and non-limiting membranes.

In an earlier work, we determined the phase diagrams of the HA-liposomes mixtures (El Kechai et al., 2017). A macrophase separation was not observed for $C > C_e$, aside from a slight syneresis for HA-Lip^+ at 2.28%. However, in HA solutions below C_e, phase separation

occurred for HA-Lip, HA-Lip^{-}, and HA-LipPEG but not for HA-Lip^{+}. In the present study, HA-liposomes were in contact with water in the vicinity of the membrane, promoting a restructuration at the microscale, leading to a macrophase separation over time. Indeed, a volume expansion of the systems was observed in the donor compartment. It indicated that water transport took place from the receptor towards the donor compartment, leading to the swelling of the hybrid systems. These fluxes were not induced by a difference in osmolality at the initial time between the donor and receptor compartments, as osmolaties were very similar (289–304 mOsm/kg versus 300 mOsm/kg). Similarly, the hydrostatic pressure did not favor water fluxes from the receptor to the donor compartment. Assuming that HA chains had not yet diffused significantly into the receptor compartment, HA was diluted from 1.5% to theoretical concentrations ranging between 0.77 and 1.12% (w/v) at V_{max} (Table 2). These HA concentrations were still in the entangled semi-dilute regime of HA. The mesh size of the HA network might be increased (from 7 to 9–12 nm), although remaining low compared to the size of the liposomes (150 nm).

Furthermore, the volume expansion of the systems depended on their capacity to release (or not) liposomes, as well as on the liposome surface (**Erreur ! Source du renvoi introuvable.** 4C). For example, HA-Lip^{+} swelled to a greater extent than HA-Lip, but lipid release was very low in both cases. It might be explained by cationic charges of liposomes not paired with anionic HA within complexes. However, the mechanism driving the swelling remains not fully understood.

Irrespective of the liposome size and surface, a volume decrease occurred after HA-liposome swelling with the non-limiting membrane (3 μm pores). It can be ascribed to an erosion mechanism. This phenomenon was strongly reduced/slowed down with the limiting membrane (0.4 μm pores) (**Erreur ! Source du renvoi introuvable.** 4B), and even completely hindered for HA-Lip^{+} during the observation period, suggesting that liposomes or/and HA migration towards the receptor compartment was responsible for the decrease in HA-liposome volume. The impact of liposome migration on the volume decrease in the donor compartment was further investigated. The volume fraction of 150 nm-liposomes at 80 mM ranged between 19 and 24%, depending on the surface characteristics of liposomes. These volume fractions were similar to other model hybrid systems studied by SANS [up to 50% (Mutch et al., 2009; Shi et al., 2016)] but higher than for other polymer-liposome mixtures evaluated in the pharmaceutical field (Billard et al., 2015; Tan et al., 2021). It permitted to convert the lipid concentration in the receptor compartment into the volume occupied by the liposomes in that compartment (open symbol in Fig. 5).

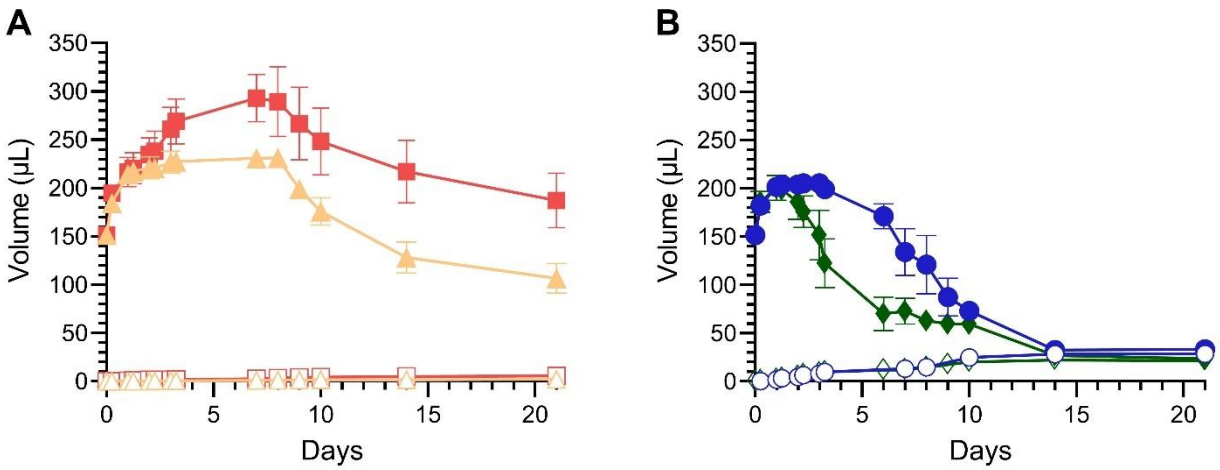

Fig. 5. Volume of HA-liposome mixtures in the donor compartment (*filled symbols*) and volume of liposomes released (calculated from liposome volume fraction) in the receptor compartment (*open symbols*) on the Transwell® model. **(**A**)** Lip: yellow, Lip^+: red. **(B)** Lip^- : green, LipPEG: blue. T = 37 °C, pore diameter of the membrane = 3 µm.

Most of the volume decrease was likely attributable to HA and related water migration for HA-Lip and HA-Lip^+ that did hardly release liposomes (Fig. 5A). Conversely, the erosion of HA-Lip^- and HA-LipPEG might to a greater part be attributable to the migration of liposomes, but this could explain just a minority of the volume decrease (Fig. 5B); thus, HA chains were likely released in that case, too.

With the 3 µm pore membrane, the departure of liposomes from the donor compartment probably weakened the system, inducing its reorganization. If the areas of aggregated liposomes were emptied from their liposomes due to migration, water could fill these zones, and locally dilute HA chains. The local viscosity might be decreased, which could further favor the erosion of the HA-liposome mixture through the release of liposomes and/or HA chain migration towards the receptor compartment. This erosion probably led to a progressive destructuring of the systems. HA chains in semi-dilute entangled solutions could move by reptation, following a movement analogous to a worm or snake (Dobrynin et al., 1995). Due to HA reptation, the mesh size might change depending on the interactions with the vesicles dispersed within the network. HA reptation towards the receptor compartment took probably of a few days in this study. This is consistent with the magnitude of reptation time (De Gennes, 1979) and the erosion mechanism of HA-LipPEG in aqueous media (Lajavardi et al., 2009). In the case of repulsive interactions (HA-Lip^- and HA-LipPEG), the swelling was limited by the rapid release of liposomes and HA reptation facilitated by liposome departure.

Conversely, attractive interactions between HA and liposomes (HA-Lip and HA-Lip^+) hindered HA reptation, which delayed the erosion and favored the swelling of the hybrid systems.

Thus, multiple mechanisms were involved in the release, including interactions between HA and liposomes, water exchanges between compartments, liposome migration, swelling and erosion of HA-liposomes, and HA reptation. Depending on the liposome surface and size, the relative importance of each mechanism was different. Furthermore, the preponderance of one mechanism over another might change during the release. Figure 6 gives a schematic depiction of these mechanisms for LipPEG and Lip^+. In the literature, theoretical models describing release kinetics have mainly been developed with non-evolving systems (Bruschi, 2015; Costa and Sousa Lobo, 2001), which was not the case in our study. Consequently, developing a mathematical model to fit the lipid release profiles was complicated. Interestingly, the release of 150 nm-LipPEG from HA using this Transwell® model agrees with in vivo data obtained with a similar formulation in Guinea pigs. Two days after the injection in the middle ear, liposomes were already visualized in the round window membrane, showing that liposomes were released (El Kechai et al., 2016). These systems delivered corticoid or antioxidant molecules into the inner ear (El Kechai et al., 2016; Jaudoin et al., 2021)

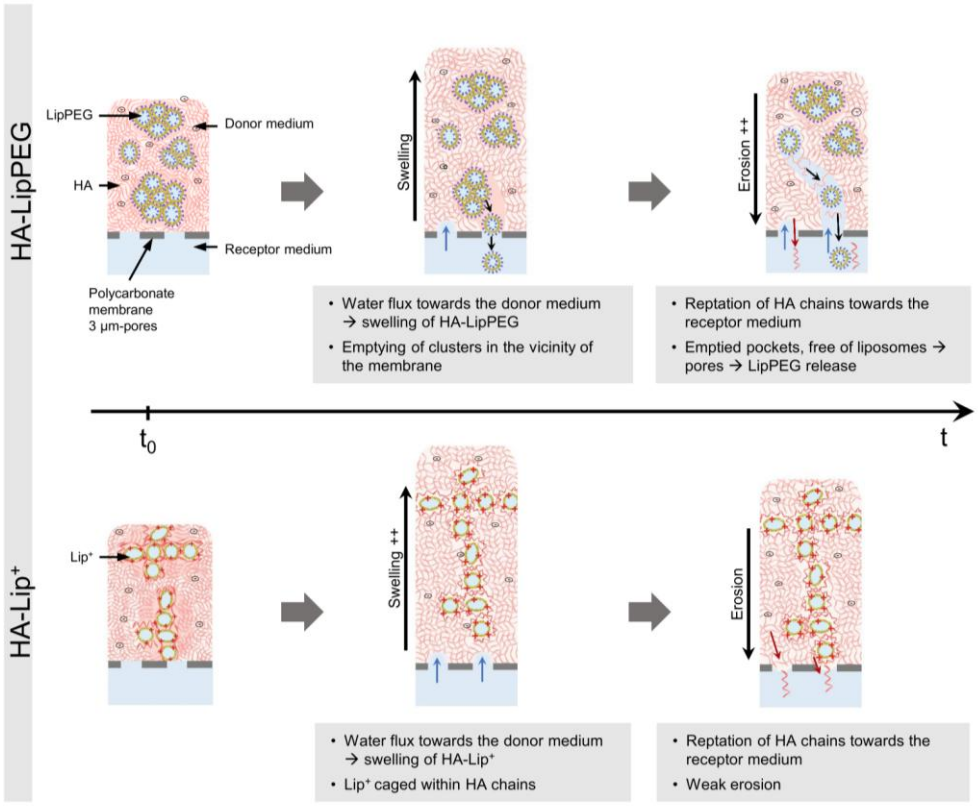

Fig. 6. Schematic depiction of the mechanisms proposed to explain the release of liposomes from HA-liposome mixtures using a Transwell® model. T = 37°C, [HA] = 1.5 % w/v, [Lipides] = 80 mM, D_h = 150 nm. Liposomes are represented as unilamellar to simplify the scheme. The microstructure at t_0 is depicted according to the results of Jaudoin et al. (2022). Blue arrows: water flux inducing swelling, red arrows: HA chain reptation, black arrows: liposome migration.

5. Conclusion

This release study was performed using a Transwell® model on complex hybrid systems, varying the liposome surface and size. Although the diameter of the liposomes was too high to be determined by SANS, the combination with cryo-EM data showed that liposomes were oligolamellar and mainly composed of two lipid bilayers. This information allowed us to calculate the liposome volume fraction (19–24%). This parameter was useful for understanding the liposome release kinetics and the volume variations of the formulations in the donor compartment over time.

Liposome surface and size impacted their release from HA-liposome hybrid systems. Multiple and complex mechanisms were involved and their relative importance over time depended on the liposome characteristics.

The HA-liposomal hybrid system appeared as a versatile formulation platform allowing different strategies for local drug delivery. The choice of liposome characteristics will depend on the selected therapeutic strategy. If liposomes are immobilized in HA entangled chains (150 nm-Lip, 150 nm-Lip^{+}, 200 and 300 nm-LipPEG), they will act as a drug reservoir and slowly release their content into the HA network. On the contrary, when liposomes migrate through the HA network (150 nm-Lip^{-}, 100 and 150 nm-LipPEG), they will be released in the biological media and potentially modify drug distribution.

The Transwell® model assesses the release of liposomes at a long timescale and is a suitable tool for discriminating formulations in vitro. It could be extended by quantifying the polymer concentration in the receptor compartment. Such model could also be applied to investigate the release of more complex hybrid systems, such as extracellular vesicles embedded within hydrogels or biomaterials.

CRediT authorship contribution statement

Céline Jaudoin: Conceptualization, Methodology, Investigation, Data curation, Formal analysis, Visualization, Writing – original draft, Writing - review & editing. **Isabelle Grillo:** Conceptualization, Methodology, Investigation, Project administration, Supervision. **Fabrice Cousin:** Investigation, Methodology, Data curation, Formal analysis, Visualization, Writing - review & editing, **Maria Maue Gehrke:** Conceptualization, Methodology, Investigation, Formal analysis. **Malika Ouldali:** Conceptualization, Methodology, Investigation, Review & editing. **Ana-Andreea Arteni:** Conceptualization, Methodology, Investigation, Review & editing. **Fanny Simelière:** Methodology, Data curation, Formal analysis, Visualization, Review & editing. **Evelyne Ferrary, Florence Siepmann, Juergen Siepmann,** Formal analysis, Visualization, Review & editing, Funding acquisition. **Amélie Bochot**: Conceptualization, Project administration, Supervision, Visualization, Writing - review & editing, Funding acquisition. **Florence Agnely**: Conceptualization, Investigation, Project administration, Supervision, Visualization, Writing - review & editing, Funding acquisition

Acknowledgements

The authors thank the Laboratoire Léon Brillouin for the beam time on PAXY instrument and Céline Jaudoin acknowledges the Ministère de l'Enseignement Supérieur, de la Recherche et de l'Innovation for her PhD grant 2017-110. This work was supported by ANR (The French National 1030 Research Agency) (N° ANR-15-CE19-0014-01, 02, 04). It also benefited from the CryoEM platform of I2BC, financed by the French Infrastructure for Integrated Structural Biology (FRISBI) [ANR-10-INSB-05-05]. The authors acknowledge Pr Luc Picton and Dr Christophe Rihouey from the Laboratoire Polymères, Biopolymères, Surfaces (PBS), UMR CNRS 6270, Normandie University for the determination of the weight average molar mass of hyaluronic acid by size exclusion chromatography coupled on-line with multiangle light scattering.

References

Agrahari, V., Agrahari, V., Mitra, A.K., 2017. Inner ear targeted drug delivery: What does the future hold? Ther. Deliv. 8, 179–184. https://doi.org/10.4155/tde-2017-0001

Bangham, A.D., Standish, M.M., Watkins, J.C., 1965. Diffusion of univalent ions across the lamellae of swollen phospholipids. J. Mol. Biol. 13, 238-IN27. https://doi.org/10.1016/S0022-2836(65)80093-6

Billard, A., Pourchet, L., Malaise, S., Alcouffe, P., Montembault, A., Ladavière, C., 2015. Liposome-loaded chitosan physical hydrogel: Toward a promising delayed-release biosystem. Carbohydr. Polym. 115, 651–657. https://doi.org/10.1016/j.carbpol.2014.08.120

Bozzuto, G., Molinari, A., 2015. Liposomes as nanomedical devices. Int. J. Nanomedicine 10, 975–999. https://doi.org/10.2147/IJN.S68861

Bruschi, M.L., 2015. Mathematical models of drug release, in: Strategies to Modify the Drug Release from Pharmaceutical Systems. Elsevier, pp. 63–86. https://doi.org/10.1016/b978-0-08-100092-2.00005-9

Costa, P., Sousa Lobo, J.M., 2001. Modeling and comparison of dissolution profiles. Eur. J. Pharm. Sci. 13, 123–133. https://doi.org/10.1016/S0928-0987(01)00095-1

Crommelin, D.J.A., van Hoogevest, P., Storm, G., 2020. The role of liposomes in clinical nanomedicine development. What now? Now what? J. Control. Release 318, 256–263. https://doi.org/10.1016/j.jconrel.2019.12.023

De Gennes, P.-G., 1979. Scaling Concepts in Polymer Physics. Cornell University Press, Ithaca, NY.

De Smedt, S.C., Lauwers, A., Demeester, J., Engelborghs, Y., De Mey, G., Du, M., 1994. Structural information on hyaluronic acid solutions as studied by probe diffusion experiments. Macromolecules 27, 141–146. https://doi.org/10.1021/ma00079a021

Dobrynin, A. V, Colby, R.H., Rubinstein, M., 1995. Scaling Theory of Polyelectrolyte Solutions. Macromolecules 28, 1859–1871. https://doi.org/10.1021/ma00110a021

El Kechai, N., Bochot, A., Huang, N., Nguyen, Y., Ferrary, E., Agnely, F., 2015. Effect of liposomes on rheological and syringeability properties of hyaluronic acid hydrogels intended for local injection of drugs. Int. J. Pharm. 487, 187–196. https://doi.org/10.1016/j.ijpharm.2015.04.019

El Kechai, N., Geiger, S., Fallacara, A., Cañero Infante, I., Nicolas, V., Ferrary, E., Huang, N., Bochot, A., Agnely, F., 2017. Mixtures of hyaluronic acid and liposomes for drug delivery: Phase behavior, microstructure and mobility of liposomes. Int. J. Pharm. 523, 246–259. https://doi.org/10.1016/j.ijpharm.2017.03.029

El Kechai, N., Mamelle, E., Nguyen, Y., Huang, N., Nicolas, V., Chaminade, P., Yen-Nicolaÿ, S., Gueutin, C., Granger, B., Ferrary, E., Agnely, F., Bochot, A., 2016. Hyaluronic acid liposomal gel sustains delivery of a corticoid to the inner ear. J. Control. Release 226, 248–257. https://doi.org/10.1016/j.jconrel.2016.02.013

Ensign, L.M., Cone, R., Hanes, J., 2014. Nanoparticle-based drug delivery to the vagina: A

review. J. Control. Release 190, 500–514. https://doi.org/10.1016/J.JCONREL.2014.04.033

Gatej, I., Popa, M., Rinaudo, M., 2004. Role of the pH on Hyaluronan Behavior in Aqueous Solution. Biomacromolecules 6, 61–67. https://doi.org/10.1021/BM040050M

Gonçalves, M., Mignani, S., Rodrigues, J., Tomás, H., 2020. A glance over doxorubicin based-nanotherapeutics: From proof-of-concept studies to solutions in the market. J. Control. Release 317, 347–374. https://doi.org/10.1016/j.jconrel.2019.11.016

Grijalvo, S., Mayr, J., Eritja, R., Díaz, D.D., 2016. Biodegradable liposome-encapsulated hydrogels for biomedical applications: A marriage of convenience. Biomater. Sci. 4, 555–574. https://doi.org/10.1039/c5bm00481k

Hua, S., de Matos, M.B.C., Metselaar, J.M., Storm, G., 2018. Current trends and challenges in the clinical translation of nanoparticulate nanomedicines: Pathways for translational development and commercialization. Front. Pharmacol. 9, 790. https://doi.org/10.3389/FPHAR.2018.00790/BIBTEX

Jaudoin, C., Grillo, I., Cousin, F., Gehrke, M., Ouldali, M., Arteni, A.A., Picton, L., Rihouey, C., Simelière, F., Bochot, A., Agnely, F., 2022. Hybrid systems combining liposomes and entangled hyaluronic acid chains: Influence of liposome surface and drug encapsulation on the microstructure. J. Colloid Interface Sci. 628, 995–1007. https://doi.org/10.1016/J.JCIS.2022.07.146

Jaudoin, C., Carré, F., Gehrke, M., Sogaldi, A., Steinmetz, V., Hue, N., Cailleau, C., Tourrel, G., Nguyen, Y., Ferrary, E., Agnely, F., Bochot, A., 2021. Transtympanic injection of a liposomal gel loaded with N-acetyl-L-cysteine: A relevant strategy to prevent damage induced by cochlear implantation in guinea pigs? Int. J. Pharm. 604, 120757. https://doi.org/10.1016/j.ijpharm.2021.120757

Kenworthy, A.K., Hristova, K., Needham, D., McIntosh, T.J., 1995. Range and magnitude of the steric pressure between bilayers containing phospholipids with covalently attached poly(ethylene glycol). Biophys. J. 68, 1921–1936. https://doi.org/10.1016/S0006-3495(95)80369-3

Kirby, B.J., Hasselbrink, E.F., 2004. Zeta potential of microfluidic substrates: 2. Data for polymers. Electrophoresis 25, 203–213. https://doi.org/10.1002/elps.200305755

Krause, W.E., Bellomo, E.G., Colby, R.H., 2001. Rheology of Sodium Hyaluronate under Physiological Conditions. Biomacromolecules 2, 65–69. https://doi.org/10.1021/bm0055798

Lajavardi, L., Camelo, S., Agnely, F., Luo, W., Goldenberg, B., Naud, M.-C., Behar-Cohen,

F., de Kozak, Y., Bochot, A., 2009. New formulation of vasoactive intestinal peptide using liposomes in hyaluronic acid gel for uveitis. J. Control. Release 139, 22–30. https://doi.org/10.1016/j.jconrel.2009.05.033

Lapčík, L., Lapčík, L., De Smedt, S., Demeester, J., Chabreček, P., 1998. Hyaluronan: Preparation, Structure, Properties, and Applications. Chem. Rev. 98. https://doi.org/10.1021/CR941199Z

Milas, M., Rinaudo, M., Roure, I., Al-Assaf, S., Phillips, G.O., Williams, P.A., 2002. Rheological behaviour of hyaluronan, healon and hylan in aqueous solutions, in: Kennedy, J.F., Phillips, G.O., Williams, P.A. (Eds.), Hyaluronan. Elsevier, pp. 181–193. https://doi.org/10.1533/9781845693121.181

Mutch, K.J., Van Duijneveldt, J.S., Eastoe, J., Grillo, I., Heenan, R.K., 2009. Testing the scaling behavior of microemulsion - Polymer mixtures. Langmuir 25, 3944–3952. https://doi.org/10.1021/la802488f

Nele, V., Holme, M.N., Kauscher, U., Thomas, M.R., Doutch, J.J., Stevens, M.M., 2019. Effect of Formulation Method, Lipid Composition, and PEGylation on Vesicle Lamellarity: A Small-Angle Neutron Scattering Study. Langmuir 35, 6064–6074. https://doi.org/10.1021/acs.langmuir.8b04256

O'Neill, H.S., Herron, C.C., Hastings, C.L., Deckers, R., Lopez Noriega, A., Kelly, H.M., Hennink, W.E., McDonnell, C.O., O'Brien, F.J., Ruiz-Hernández, E., Duffy, G.P., 2017. A stimuli responsive liposome loaded hydrogel provides flexible on-demand release of therapeutic agents. Acta Biomater. 48, 110–119. https://doi.org/10.1016/j.actbio.2016.10.001

Ritger, P.L., Peppas, N.A., 1987. A simple equation for description of solute release I. Fickian and non-fickian release from non-swellable devices in the form of slabs, spheres, cylinders or discs. J. Control. Release 5, 23–36. https://doi.org/10.1016/0168-3659(87)90034-4

Scott, J.E., 2007. Secondary Structures in Hyaluronan Solutions: Chemical and Biological Implications, in: Evered, D., Whelan, J. (Eds.), Ciba Foundation Symposium 143 - The Biology of Hyaluronan, Novartis Foundation Symposia. John Wiley & Sons, Ltd, pp. 6–20. https://doi.org/10.1002/9780470513774.ch2

Shah, S., Dhawan, V., Holm, R., Nagarsenker, M.S., Perrie Y., 2020. Liposomes: Advancements and innovation in the manufacturing process. Adv Drug Deliv Rev 154-155, 102-122. https://doi: 10.1016/j.addr.2020.07.002

Shi, L., Carn, F., Boué, F., Buhler, E., 2016. Role of the ratio of biopolyelectrolyte persistence

length to nanoparticle size in the structural tuning of electrostatic complexes. Phys. Rev. E 94, 032504. https://doi.org/10.1103/PhysRevE.94.032504

Taglienti, A., Cellesi, F., Crescenzi, V., Sequi, P., Valentini, M., Tirelli, N., 2006. Investigating the interactions of hyaluronan derivatives with biomolecules. The use of diffusional NMR techniques. Macromol. Biosci. 6, 611–622. https://doi.org/10.1002/mabi.200600041

Tan, C., Wang, J., Sun, B., 2021. Biopolymer-liposome hybrid systems for controlled delivery of bioactive compounds: Recent advances. Biotechnol. Adv. 48, 107727. https://doi.org/10.1016/j.biotechadv.2021.107727

Uchegbu, I.F., Siew, A., 2013. Nanomedicines and nanodiagnostics come of age. J. Pharm. Sci. 102, 305–310. https://doi.org/10.1002/jps.23377

Wang, Y., Ren, J., Lu, Y., Yin, T., Xie, D., 2012. Evaluation of intratympanic dexamethasone for treatment of refractory sudden sensorineural hearing loss. J. Zhejiang Univ. Sci. B 13, 203–208. https://doi.org/10.1631/jzus.B1100248